

# Synthesis of CD<sub>3</sub>-Labeled 11-*cis*-Retinals and Application to Solid-State Deuterium NMR Spectroscopy of Rhodopsin<sup>#</sup>

Katsunori Tanaka,<sup>1,†</sup> Andrey V. Struts,<sup>2</sup> Sonja Krane,<sup>1,††</sup>  
Naoko Fujioka,<sup>1,†††</sup> Gilmar F. J. Salgado,<sup>3,††††</sup> Karina Martínez-Mayorga,<sup>2</sup>  
Michael F. Brown,<sup>\*2,3</sup> and Koji Nakanishi<sup>1</sup>

<sup>1</sup>Department of Chemistry, Columbia University, New York, New York 10027, USA

<sup>2</sup>Department of Chemistry, University of Arizona, Tucson, Arizona 85721, USA

<sup>3</sup>Department of Biochemistry & Molecular Biophysics, University of Arizona, Tucson, Arizona 85721, USA

Received January 9, 2007; E-mail: mfbrown@u.arizona.edu

Efficient synthesis of 11-*Z*-retinals labeled with <sup>2</sup>H at the C5, C9, or C13 methyl groups is described. The <sup>2</sup>H-labeled retinals were used to regenerate the visual pigment rhodopsin for structural investigations. Solid-state <sup>2</sup>H NMR data provided the orientation of retinal within the rhodopsin binding pocket as well as its conformation. Extension of the approach to other membrane receptors can yield knowledge of their mechanisms of activation as a guide for ligand-based drug design.

Site-directed nuclear spin labeling in combination with solid-state NMR spectroscopy can give unique information regarding the conformation and orientation of ligands bound to integral membrane proteins and G protein-coupled receptors such as rhodopsin. Biomolecular applications of NMR typically rely on the availability of suitable isotopically labeled compounds. Effectively, two strategies are possible: either the molecules are uniformly labeled, e.g. with <sup>13</sup>C, <sup>15</sup>N, or <sup>2</sup>H isotopes through bacterial expression in the case of proteins,<sup>1–4</sup> or rather organic synthesis is used to introduce isotopic labels to probe specific regions of interest within the molecule.<sup>5,6</sup> For solid-state NMR spectroscopy of biomolecules specific labeling is often used.<sup>7–9</sup> Deuterium substitution in the case of <sup>2</sup>H NMR is widely applicable to membrane lipids,<sup>10,11</sup> membrane proteins,<sup>7,12</sup> and nucleic acids.<sup>13,14</sup> Another important application of <sup>2</sup>H-isotope labeling involves neutron diffraction of membrane lipids<sup>15</sup> and membrane proteins.<sup>16,17</sup> Organic synthesis<sup>6,18–20</sup> has been applied extensively to <sup>13</sup>C and <sup>2</sup>H labeling of retinal for solid-state NMR applications to bacteriorhodopsin<sup>21–23</sup> or rhodopsin.<sup>8,24,25</sup> In view of the biological importance of retinal, it is desirable that additional synthetic methods for <sup>2</sup>H-isotope labeling are described. We report herein the efficient synthesis of deuterated retinals having methyl <sup>2</sup>H isotope labels, namely, 11-*Z*-[5-CD<sub>3</sub>]-, 11-*Z*-

[9-CD<sub>3</sub>]-, and 11-*Z*-[13-CD<sub>3</sub>]-retinals (structures shown in Fig. 1). Deuterium labeling enables us to obtain site-specific orientational restraints to model the structure of retinal bound to rhodopsin and other photoreceptors in combination with bioorganic and biophysical data.

## Results and Discussion

**Synthesis of 11-*cis*-Retinals Deuterated at C5, C9, and C13 Methyl Groups.** The stereoselective synthesis of deuterated retinals, namely, 11-*Z*-[5-CD<sub>3</sub>]-retinal, 11-*Z*-[9-CD<sub>3</sub>]-retinal, and 11-*Z*-[13-CD<sub>3</sub>]-retinal was carried out by the Ito's procedure, which utilizes the diene/tricarbonyliron complex (Schemes 1–3).<sup>19</sup> Other methods for the preparation of <sup>2</sup>H-labeled retinals have been described previously.<sup>26,27</sup> For synthesis of [5-CD<sub>3</sub>]- and [9-CD<sub>3</sub>]-retinals, the regioselectively deuterated  $\beta$ -ionones **4** and **7** were used as the starting materials and were prepared according to Scheme 1. Thus, 2,2-dimethylcyclohexanone (**1**) was reacted with CD<sub>3</sub>I where lithium diisopropylamide (LDA) was used as a base to provide **2** in 80% yield, which was converted to the triflate **3** by treatment with LDA and *N*-phenylbis(trifluoromethanesulfonimide) (NPhTf<sub>2</sub>) in 65% yield. The triflate **3** was then subjected to the Heck reaction with methylvinylketone in the presence of PdCl<sub>2</sub>(PPh<sub>3</sub>)<sub>2</sub> in DMF, providing the [5-CD<sub>3</sub>]- $\beta$ -ionone (**4**) in 50% yield. Alternatively, the  $\beta$ -ionone was treated with bromine and sodium hydroxide in 1,4-dioxane to give the acid **5** in 88% yield, which was converted to the Weinreb amide **6** by reaction with methoxymethylamine hydrochloride in the presence of DMAP and EDC in 89% yield. The amide **6** was successfully treated with deuterated methylmagnesium iodide (CD<sub>3</sub>MgI) in THF to yield [9-CD<sub>3</sub>]- $\beta$ -ionone (**7**) in 66% yield.

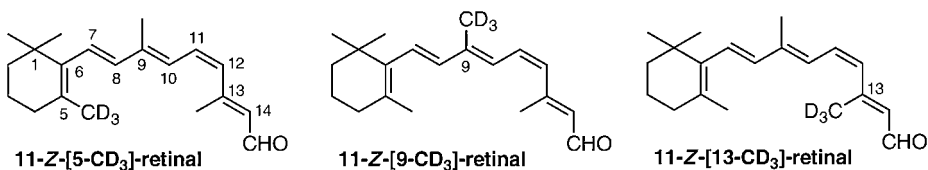
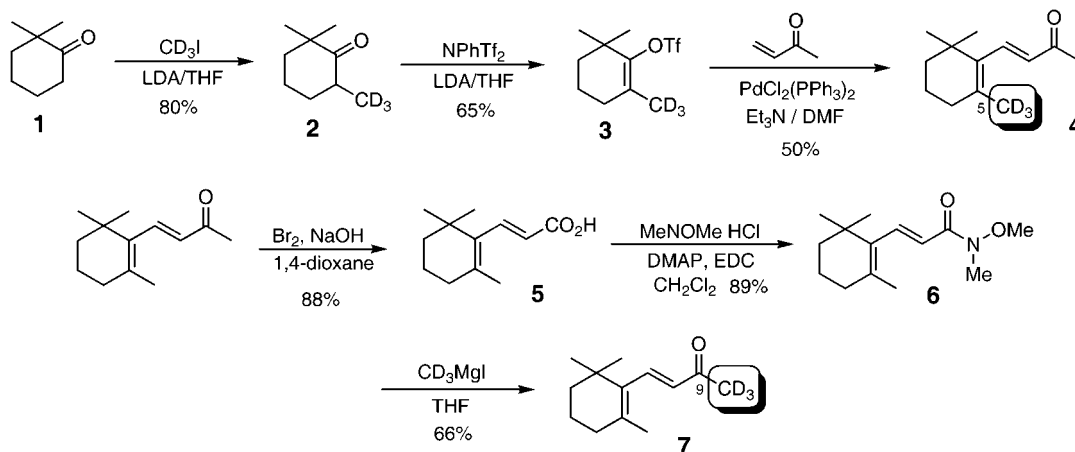
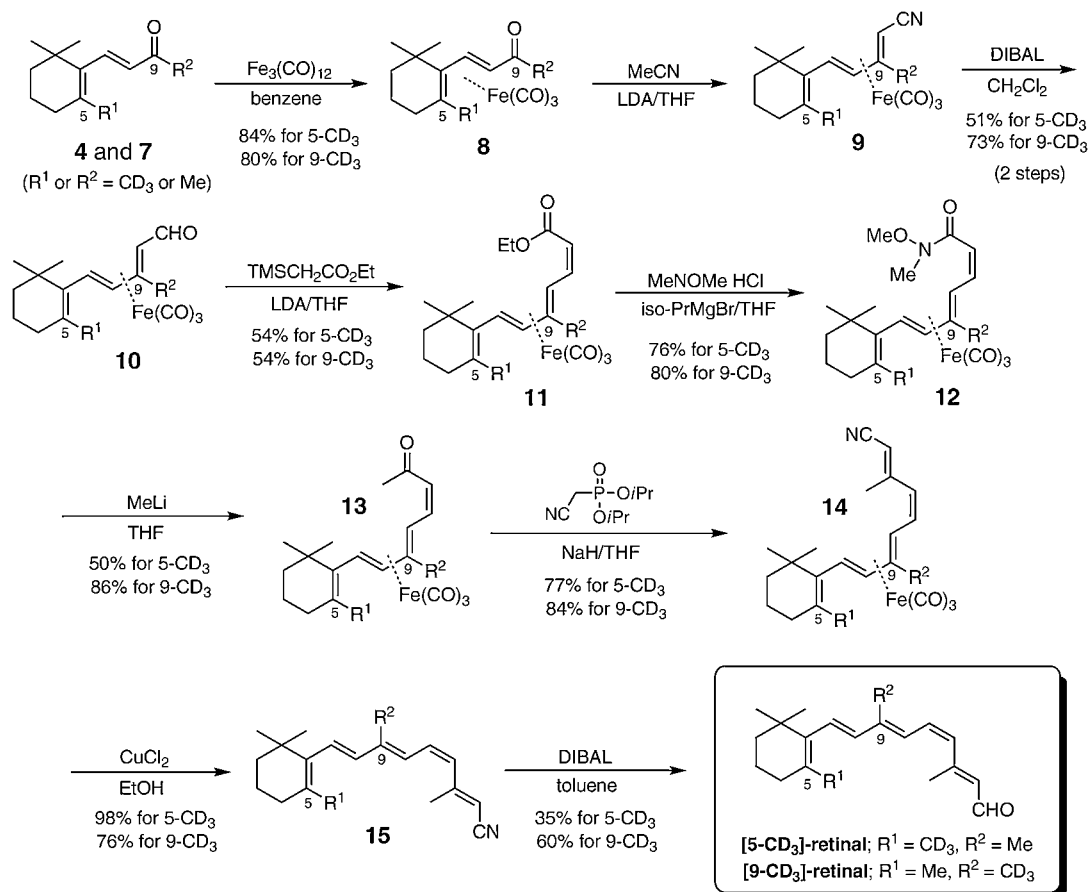
The [5-CD<sub>3</sub>]- and [9-CD<sub>3</sub>]- $\beta$ -ionones (**4** and **7**), prepared in Scheme 1, were respectively converted to the diene/tricarbonyliron complex **8** by treatment with triirondodecacarbonyl

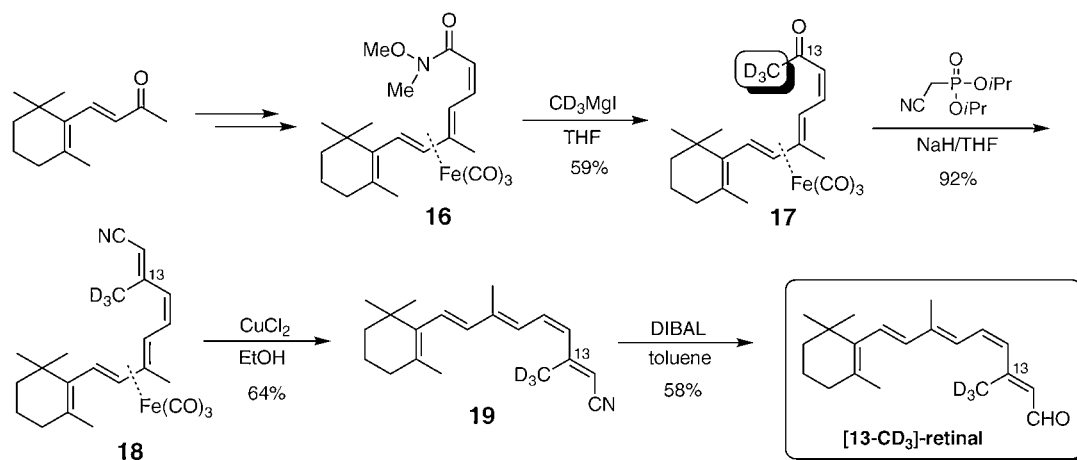
<sup>†</sup> Present address: Department of Chemistry, Graduate School of Science, Osaka University, 1-1 Machikaneyama, Toyonaka, Osaka 560-0043

<sup>††</sup> Present address: Publications Division, American Chemical Society, Washington, DC 20036, USA

<sup>†††</sup> Present address: Shionogi & Co., Ltd., Osaka

<sup>††††</sup> Present address: Faculté de Pharmacie, Université René Descartes, Paris 75270, France

Fig. 1. 11-Z-[5-CD<sub>3</sub>]-, 11-Z-[9-CD<sub>3</sub>]-, and 11-Z-[13-CD<sub>3</sub>]-retinals.Scheme 1. Synthesis of [5-CD<sub>3</sub>]- and [9-CD<sub>3</sub>]-β-ionones.Scheme 2. Synthesis of 11-Z-[5-CD<sub>3</sub>]- and 11-Z-[9-CD<sub>3</sub>]-retinals.

Scheme 3. Synthesis of 11-Z-[13-CD<sub>3</sub>]-retinal.

(Fe<sub>3</sub>(CO)<sub>12</sub>) in hot benzene (Scheme 2). The iron complex **8** was alkylated with the lithium salt of acetonitrile in THF, which was subsequently reduced by diisobutylaluminum hydride (DIBAL) to provide the (*E*)-conjugated aldehyde **10** stereoselectively, with the concomitant shift of the tricarbonyl-iron group to the C7–C8/C9–10 diene. Stereoselective transformation to the *Z*-ester **11** was achieved by Peterson olefination with ethyl trimethylsilylacetate, by virtue of the steric bulkiness of the tricarbonyliron moiety,<sup>19</sup> which was then converted to the Weinreb amide **12** by reaction with *iso*-propylmagnesium bromide and methoxymethylamine in THF. Alkylation of the amide **12** with methyl lithium in THF and *E*-selective Horner–Emmons reaction with diisopropyl cyanomethylphosphonate and sodium hydride gave the nitrile **14**. Demetalation was realized upon treatment with copper(II) dichloride in ethanol. Finally, DIBAL reduction of the nitrile **15** followed by purification by silica-gel chromatography provided the 11-Z-[5-CD<sub>3</sub>]-retinal and 11-Z-[9-CD<sub>3</sub>]-retinal, respectively.

Similarly, the 11-Z-[13-CD<sub>3</sub>]-retinal (Scheme 3) was synthesized from the Weinreb amide **16**, stereoselectively prepared from the  $\beta$ -ionone via the same sequences of the reactions shown in Scheme 1. In order to incorporate the CD<sub>3</sub> moiety at the C13 position, the amide **16** was alkylated with CD<sub>3</sub>MgI in 59% yield. Subsequent Horner–Emmons reaction (92%), demetalation (64%), and DIBAL reduction (58%) successfully provided the desired 11-Z-[13-CD<sub>3</sub>]-retinal. All three CD<sub>3</sub>-labeled 11-*cis*-retinals thus prepared were stereochemically pure, and required no further HPLC purification.

The synthetic 11-Z-[5-CD<sub>3</sub>]-, 11-Z-[9-CD<sub>3</sub>]-, and 11-Z-[13-CD<sub>3</sub>]-retinals were stored in benzene solution at –70 °C in total darkness. They were characterized by their UV–visible spectra, Fourier transform infrared spectra, and their <sup>1</sup>H, <sup>2</sup>H, and <sup>13</sup>C NMR spectra (see Experimental Section). The deuterium content of the synthetic deuterated retinal samples was confirmed by <sup>2</sup>H NMR spectroscopy, and each gave a single peak in benzene solution. Mass spectrometry in acetone/acetonitrile using positive electrospray ionization (ESI) further confirmed the purity of the synthetic deuterated retinals. For the 11-Z-[5-CD<sub>3</sub>]- and 11-Z-[13-CD<sub>3</sub>]-retinals, the (quasi)-molecular MH<sup>+</sup> ions were at *m/z* = 288.1, consistent with a single-deuterated methyl group, as compared with authentic

11-Z-retinal with MH<sup>+</sup> at *m/z* = 285.1. (The molar mass of protiated retinal is 284.4). However, for 11-Z-[9-CD<sub>3</sub>]-retinal, the ESI mass spectrum gave four peaks at *m/z* = 288.1, 287.2, 286.1, and 285.1/285.3. Hence, it is possible that some exchange of deuterium occurred to yield retinal isotopomers with CD<sub>3</sub>, CHD<sub>2</sub>, CH<sub>2</sub>D, or CH<sub>3</sub> groups.

#### Application to <sup>2</sup>H NMR Spectroscopy of Rhodopsin.

Deuterium NMR in combination with site-directed <sup>2</sup>H-nuclear spin labeling provides structural information for ligands bound to integral membrane proteins such as rhodopsin, and is complementary to X-ray crystallographic studies. An advantage of solid-state NMR is that single crystals are unnecessary, and moreover dynamical information is available.<sup>10</sup> We applied solid-state <sup>2</sup>H NMR spectroscopy to investigate the conformation and orientation of retinal within rhodopsin as a prototype for G protein-coupled receptors (GPCRs). This knowledge is broadly significant for GPCR biology and pharmacology in general. More specifically, the nature of the primary photochemical events involving rhodopsin is crucial for understanding the process of visual signaling.<sup>28,29</sup>

We conducted studies of the synthetic CD<sub>3</sub>-labeled retinals covalently bound to rhodopsin in bilayer membranes using solid-state NMR spectroscopy (Fig. 2). This procedure involved the regeneration of rhodopsin with 11-Z-[5-CD<sub>3</sub>]-, 11-Z-[9-CD<sub>3</sub>]-, or 11-Z-[13-CD<sub>3</sub>]-retinal prepared by organic synthesis. Rhodopsin was then purified and recombined with 1-palmitoyl-2-oleoyl-*sn*-glycero-3-phosphocholine (POPC) (1:50 molar ratio) by detergent dialysis.<sup>30</sup> Membranes containing 11-Z-[5-CD<sub>3</sub>]-retinylidene rhodopsin, 11-Z-[9-CD<sub>3</sub>]-retinylidene rhodopsin, or 11-Z-[13-CD<sub>3</sub>]-retinylidene rhodopsin embedded in a POPC bilayer were macroscopically aligned on planar glass substrates by isopotential ultracentrifugation.<sup>25</sup> Deuterium NMR lineshapes were then measured for the C5, C9, or C13 deuterated methyl substituents of the retinylidene ligand to elucidate the orientation, conformation, and mobility of the chromophore of rhodopsin.

Solid-state <sup>2</sup>H NMR spectra for rhodopsin containing retinal specifically <sup>2</sup>H-labeled at the C5, C9, or C13 methyl groups in aligned membrane bilayers are displayed in Figs. 2a–2c, respectively. Comparison of the <sup>2</sup>H NMR spectra for the C9 methyl group in Fig. 2b to the corresponding spectra for the C5 and C13 methyl groups in Figs. 2a and 2c indicates that

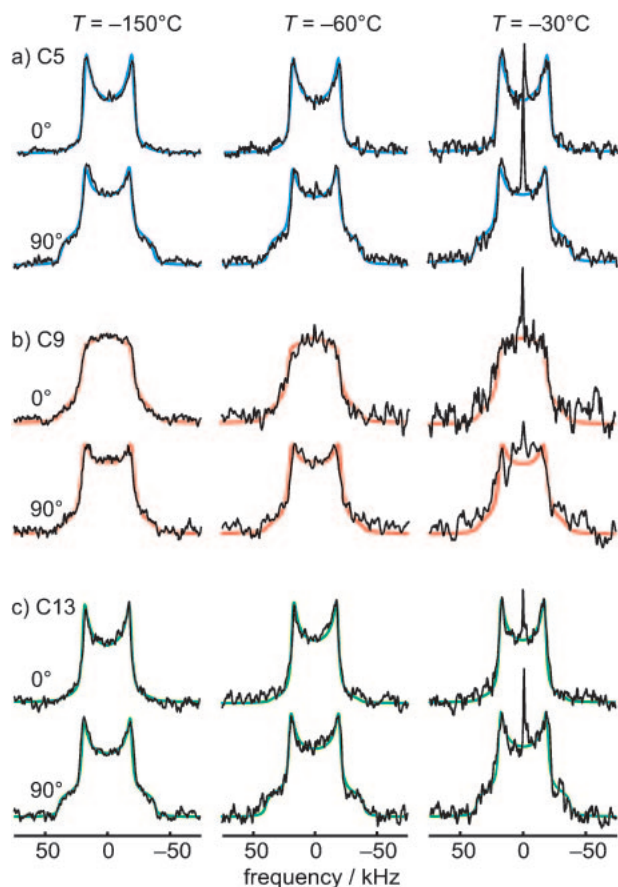


Fig. 2. Solid-state  $^2\text{H}$ NMR spectra of retinal ligand bound to rhodopsin in aligned membranes at 76.8 MHz (11.7 T) in the dark state. Data are shown for (a) 11-*Z*-[5- $\text{CD}_3$ ]-retinylidene rhodopsin, (b) 11-*Z*-[9- $\text{CD}_3$ ]-retinylidene rhodopsin, and (c) 11-*Z*-[13- $\text{CD}_3$ ]-retinylidene rhodopsin, i.e. with 11-*cis*-retinal deuterated at the C5, C9, or C13 methyl groups, respectively, at temperatures of  $-150^\circ\text{C}$ ,  $-60^\circ\text{C}$ , and  $-30^\circ\text{C}$ .  $^2\text{H}$ NMR spectra were acquired for rhodopsin/POPC recombinant membranes (1:50 molar ratio) with the membrane normal aligned at  $\theta = 0$  and  $90^\circ$  relative to the main magnetic field  $\mathbf{B}_0$ . Samples nominally contained 5 mM HEPES buffer prepared with  $^2\text{H}$ -depleted  $^1\text{H}_2\text{O}$  at pH 6.8.

the intensity as revealed by the signal-to-noise ratio is substantially less, despite the greater number of scans. We ascribe this to incomplete deuteration of the C9 methyl substituent (see above), together with a relatively long spin-lattice relaxation time ( $T_{1\rho}$ ; not shown); both require longer spectral acquisitions versus the other two positions. The solid-state  $^2\text{H}$ NMR spectra reveal that the methyl substituents undergo rapid three-fold rotation at all temperatures. The orientation-dependent line-shapes are related to the angles that the three-fold symmetry axes of the different methyl groups make to the membrane surface normal.<sup>31</sup> In addition, the  $^2\text{H}$ NMR spectra in Fig. 2 are relatively constant from  $-150$  to  $-60^\circ\text{C}$ , which demonstrates the stability of the retinal conformation over a wide temperature range. This lack of temperature variation of the methyl group orientations is important with regard to X-ray crystallographic studies of rhodopsin and its photointermediates, which are typically conducted at cryogenic temperatures.<sup>32,33</sup>

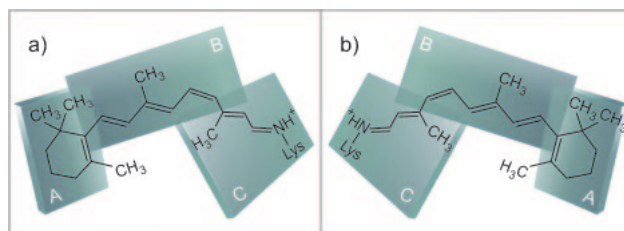


Fig. 3. Structures for 11-*cis*-retinal in the dark state of rhodopsin calculated from orientational  $^2\text{H}$ NMR constraints and  $^{13}\text{C}$ NMR distance restraints. Enantiomeric structures (a) and (b) are related by a vertical symmetry plane. The right-hand structure (b) is excluded based on circular dichroism results (see text).

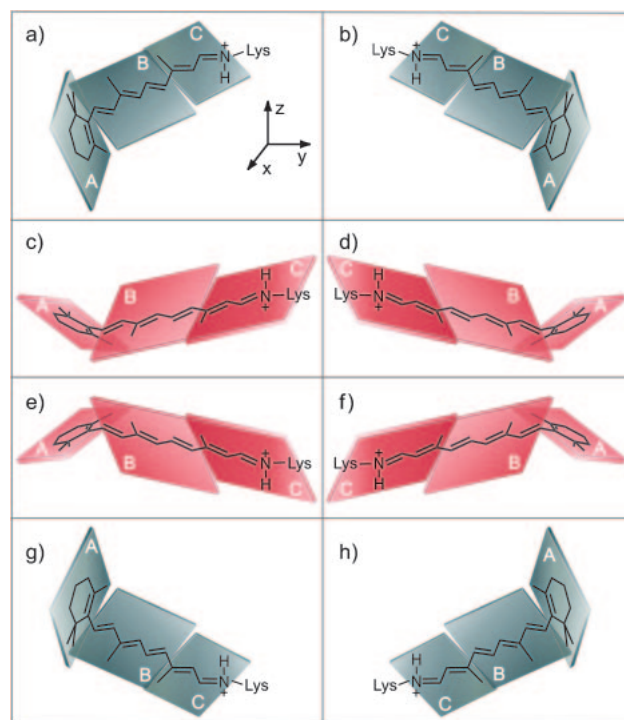


Fig. 4. Structural solutions for *trans* retinal within the binding pocket of rhodopsin in the meta I state. Angular restraints are provided by simulating the  $^2\text{H}$ NMR data for the C5, C9, and C13 methyl groups together with linear dichroism results in terms of a simple three-plane model. Structures (a), (b), (g), (h) shown in green, and (c), (d), (e), (f) in red, are obtained from each other by reflection symmetry transformations. Only the top left structure (a) and its mirror image (b) are consistent with electron crystallographic data.

We derived two possible structures for retinal in the dark state based on the angular restraints from  $^2\text{H}$ NMR (Fig. 3).<sup>34</sup> However, circular dichroism studies of locked retinoids imply that the twist is positive for the  $\text{C11}=\text{C12}-\text{C13}=\text{C14}$  dihedral angle,<sup>35</sup> whereas it is negative for the  $\text{C5}=\text{C6}-\text{C7}=\text{C8}$  angle.<sup>36</sup> This leaves as the only plausible physical structure the one shown in Fig. 3a. In the meta I state of bleached rhodopsin, eight possible solutions are obtained from the orientational  $^2\text{H}$ NMR and distance  $^{13}\text{C}$ NMR restraints (Fig. 4).<sup>37</sup> The solutions in Figs. 4c–4h can be eliminated, since based on electron

crystallography the position of the  $\beta$ -ionone ring in meta I remains the same as in the ground state.<sup>38</sup> Molecular modeling<sup>34</sup> also reveals that the conformation in Fig. 4b is less likely due to steric hindrance within the binding pocket of rhodopsin. As a result, the structure in Fig. 4a is the most plausible for retinal in the meta I state, having a negative dihedral angle of  $-32^\circ$  for the C6–C7 bond. This conclusion is consistent with measurements of the C8-to-C17 and C8-to-C18 distances in meta I.<sup>39</sup>

Investigations of rhodopsin with a bound  $^2\text{H}$ -labeled ligand open the door to application of  $^2\text{H}$ NMR to study the conformation, orientation, and dynamics of retinal in the dark state,<sup>25</sup> where the ligand is 11-*cis*, as well as the meta I state with an all-*trans* polyene chain (see Appendix).<sup>11,37</sup> The angular-dependent  $^2\text{H}$ NMR lineshapes for deuterated retinal yield the orientation of the labeled C–CD<sub>3</sub> methyl group axes relative to the membrane normal, which cannot be obtained with other biophysical techniques.<sup>10</sup> Thus,  $^2\text{H}$ NMR provides angular information for the retinylidene bond orientations that can be combined with constraints about the geometry of the molecule, and with the results of other biophysical,<sup>39–43</sup> bioorganic,<sup>35,36</sup> and biochemical<sup>44</sup> methods. In particular,  $^2\text{H}$ NMR data can be used to refine the results of X-ray and electron diffraction studies of rhodopsin in the dark state<sup>32,45–47</sup> and its photo-intermediates.<sup>32,33,38</sup> Moreover, apart from giving information complementary to other techniques, using  $^2\text{H}$ NMR rhodopsin can be studied in a native-like membrane bilayer environment, in contrast to X-ray diffraction studies of single crystals<sup>32,45,47</sup> or electron diffraction of 2-D crystals.<sup>38</sup> Last, we note that we obtain information about the retinal ligand in the meta I state, which is currently unavailable from X-ray crystallography.

### Conclusion

Our findings illustrate how specific  $^2\text{H}$ -isotopic labeling can be used in conjunction with solid-state  $^2\text{H}$ NMR spectroscopy to investigate ligands bound to GPCRs and other membrane proteins. As a specific example, we have focused on the visual receptor rhodopsin. Additional GPCRs and ligand-gated ion channels are attractive pharmaceutical targets. Organic synthesis of  $^2\text{H}$ -labeled retinoids together with solid-state  $^2\text{H}$ NMR spectroscopy gives unique information about the local environment of ligands in GPCRs such as rhodopsin. Experimental  $^2\text{H}$ NMR data and theoretical lineshape analysis yield the conformation of the retinal ligand, and show how it is oriented within the binding cavity of rhodopsin in the membrane-bound state. This knowledge is pertinent to investigating the molecular basis for the pharmacology of agonists and antagonists in terms of receptor activation. Extension of this approach to other receptors can facilitate ligand-based drug discovery and the design of new pharmaceutical agents.

### Experimental

**Materials and Methods.** Synthesis of 11-Z-[5-CD<sub>3</sub>]-, 11-Z-[9-CD<sub>3</sub>]-, and 11-Z-[13-CD<sub>3</sub>]-retinals followed reported procedures.<sup>19</sup> Anhydrous dichloromethane, diethylether, benzene, and acetonitrile were dried and distilled. Unless otherwise noted, materials were obtained from a commercial supplier and were used without further purification. All reactions were performed in pre-dried glassware under Ar. Purification was performed either by column chromatography using ICN silica gel (32–63 mesh) or

by preparative TLC using silica-gel plates, 60 F-254, 0.25 mm (E. Merck).  $^1\text{H}$ NMR spectra were acquired with a Bruker DMX 400 MHz spectrometer and were referred in parts per million (ppm) to TMS ( $\delta$ ), with coupling constants ( $J$ ) in Hertz (Hz). Proton decoupled  $^{13}\text{C}$  spectra were obtained with a Bruker DRX 600 spectrometer and chemical shifts were referenced to the CDCl<sub>3</sub> solvent peak at 77.0 ppm. Assignments were made by comparison with published retinal  $^{13}\text{C}$  chemical shifts.<sup>48,49</sup> The  $^{13}\text{C}$  peaks originating from 5-CD<sub>3</sub>, 9-CD<sub>3</sub>, or 13-CD<sub>3</sub> groups were not observed due to heteronuclear  $^{13}\text{C}$ – $^2\text{H}$  coupling confirming the low abundance of residual non-deuterated methyl groups. High-resolution  $^2\text{H}$ NMR spectra were obtained with a Bruker DRX 400 spectrometer and each of the compounds in benzene gave a single peak assigned to the deuterated CD<sub>3</sub> groups. ESI mass spectra were measured in acetone/acetonitrile using positive electrospray ionization with a JEOL HX110A high-resolution mass spectrometer.

**11-Z-[5-CD<sub>3</sub>]-Retinal:**  $^1\text{H}$ NMR (400 MHz, CDCl<sub>3</sub>)  $\delta_{\text{H}}$  1.07 (s, 6H), 1.43–1.46 (m, 2H), 1.52–1.59 (m, 2H), 1.74 (s, 3H), 1.76 (d, 3H,  $J = 1.2$  Hz), 1.91 (ddd, 2H,  $J = 6.4, 6.4, 1.6$  Hz), 5.59 (d, 1H,  $J = 12.0$  Hz), 6.10 (d, 1H,  $J = 7.6$  Hz), 6.21 (d, 1H,  $J = 16.0$  Hz), 6.34 (d, 1H,  $J = 16.0$  Hz), 6.38 (dd, 1H,  $J = 12.0, 12.0$  Hz), 6.58 (d, 1H,  $J = 12.0$  Hz), 9.90 (d, 1H,  $J = 7.8$  Hz);  $^{13}\text{C}$ NMR (150.9 MHz, CDCl<sub>3</sub>)  $\delta_{\text{C}}$  13.0 (9-CH<sub>3</sub>), 13.1 (13-CH<sub>3</sub>), 19.1 (C3), 29.0 (1,1-CH<sub>3</sub>), 33.1 (C4), 34.2 (C1), 39.7 (C2), 125.5 (C10), 129.0 (C7 or C12), 129.4 (C12 or C7), 129.7 (C14), 132.5 (C11), 134.5 (C10, from all-*trans* retinal), 137.0 (C6 or C8), 137.6 (C8 or C6), 141.2 (C9), 154.7 (C13), 191.1 (C15); ESI-MS (positive)  $m/z$  288.1 [(M + H)<sup>+</sup>].

**11-Z-[9-CD<sub>3</sub>]-Retinal:**  $^1\text{H}$ NMR (400 MHz, CDCl<sub>3</sub>)  $\delta_{\text{H}}$  1.10 (s, 6H), 1.42–1.45 (m, 2H), 1.54–1.59 (m, 2H), 1.67 (s, 3H), 1.77 (s, 3H), 1.91 (dd, 2H,  $J = 6.2, 6.2$  Hz), 5.58 (d, 1H,  $J = 11.8$  Hz), 6.09 (d, 1H,  $J = 7.8$  Hz), 6.20 (d, 1H,  $J = 16.0$  Hz), 6.32 (d, 1H,  $J = 16.0$  Hz), 6.37 (dd, 1H,  $J = 11.9, 11.9$  Hz), 6.57 (d, 1H,  $J = 12.4$  Hz), 9.90 (d, 1H,  $J = 7.8$  Hz);  $^{13}\text{C}$ NMR (150.9 MHz, CDCl<sub>3</sub>)  $\delta_{\text{C}}$  13.1 (13-CH<sub>3</sub>), 19.1 (C3), 21.8 (5-CH<sub>3</sub>), 29.0 (1,1-CH<sub>3</sub>), 33.1 (C4), 34.2 (C1), 39.7 (C2), 125.5 (C10), 129.0 (C7 or C12), 129.4 (C12 or C7), 129.7 (C14), 130.5 (C5), 132.5 (C11), 134.5 (C10, all-*trans* retinal), 137.0 (C6 or C8), 137.6 (C8 or C6), 154.7 (C13), 191.1 (C15); ESI-MS (positive)  $m/z$  288.1 [(M + H)<sup>+</sup>].

**11-Z-[13-CD<sub>3</sub>]-Retinal:**  $^1\text{H}$ NMR (400 MHz, CDCl<sub>3</sub>)  $\delta_{\text{H}}$  1.07 (s, 6H), 1.43–1.46 (m, 2H), 1.53–1.59 (m, 2H), 1.68 (s, 3H), 1.74 (s, 3H), 1.91 (dd, 2H,  $J = 6.1, 6.1$  Hz), 5.59 (d, 1H,  $J = 11.8$  Hz), 6.10 (d, 1H,  $J = 7.7$  Hz), 6.21 (d, 1H,  $J = 16.0$  Hz), 6.33 (d, 1H,  $J = 15.7$  Hz), 6.38 (dd, 1H,  $J = 11.9, 11.9$  Hz), 6.57 (d, 1H,  $J = 12.4$  Hz), 9.90 (d, 1H,  $J = 7.8$  Hz);  $^{13}\text{C}$ NMR (150.9 MHz, CDCl<sub>3</sub>)  $\delta_{\text{C}}$  13.0 (9-CH<sub>3</sub>), 19.1 (C3), 21.8 (5-CH<sub>3</sub>), 29.0 (1,1-CH<sub>3</sub>), 33.1 (C4), 34.2 (C1), 39.7 (C2), 125.5 (C10), 129.0 (C7 or C12), 129.4 (C12 or C7), 129.7 (C14), 130.5 (C5), 132.5 (C11), 134.5 (C10, all-*trans* retinal), 137.0 (C6 or 8), 137.6 (C8 or C6), 141.2 (C9), 191.1 (C15); ESI-MS (positive)  $m/z$  288.1 [(M + H)<sup>+</sup>].

**Preparation of  $^2\text{H}$  Retinylidene Rhodopsin in POPC Membranes.** All procedures involving rhodopsin were carried out under dim red light or in total darkness at 4 °C unless otherwise specified. Rhodopsin-containing membranes were isolated from frozen bovine retinas (W. L. Lawson Co., Lincoln, NE) as described.<sup>30</sup> Suspensions of rod outer segment (ROS) membranes in 10 mM HEPES buffer at pH 6.8 containing 100 mM hydroxylamine were bleached for 30 min at 4 °C, using yellow light. Well-homogenized suspensions were prepared and gently handled using a Pasteur pipette. The opsin-containing membranes thus obtained were centrifuged for 30 min at 20000 rpm in a Sorvall T865 rotor

(40660  $\times$  g) at 4 °C, after which the pellet was resuspended in 10 mM HEPES buffer without hydroxylamine, repeating the procedure 4 $\times$ . Benzene solutions containing the synthetic 11-Z-[5-CD<sub>3</sub>]-retinal, 11-Z-[9-CD<sub>3</sub>]-retinal, or 11-Z-[13-CD<sub>3</sub>]-retinal were evaporated using a light stream of N<sub>2</sub>, after which retinal was re-dissolved in EtOH (maximum of 1% v/v with respect to buffer). Synthetic retinal was immediately added to opsin-containing membranes in 1.5 molar excess, and regeneration was carried out for 1.5 h at 37 °C. Rhodopsin was dissolved in dodecyltrimethylammonium bromide (DTAB) detergent and was purified on a hydroxyapatite column. The regenerated rhodopsin was then recombined with 1-palmitoyl-2-oleoyl-*sn*-glycero-3-phosphocholine (POPC) in a 1:50 protein/lipid molar ratio by detergent dialysis.<sup>30</sup>

**Solid-State <sup>2</sup>H NMR Spectroscopy.** Membranes containing 11-Z-[5-CD<sub>3</sub>]-retinylidene rhodopsin, 11-Z-[9-CD<sub>3</sub>]-retinylidene rhodopsin, or 11-Z-[13-CD<sub>3</sub>]-retinylidene rhodopsin and POPC (1:50) were aligned on planar glass substrates by isopotential ultracentrifugation.<sup>25,50</sup> Recombinant membranes with rhodopsin nominally in 5 mM HEPES buffer at pH 6.8 were subjected to slow evaporation under a nitrogen atmosphere at 4 °C. The glass plates containing the recombinant membranes as a dry film were hydrated in a sealed container, containing a saturated salt solution (NaBr in <sup>2</sup>H-depleted water) with a relative humidity  $\approx$ 63% at 4 °C. Thereafter, 25 glass plates were stacked and inserted in a cut-off 8  $\times$  22 mm NMR tube sealed with a Teflon plug. Recombinant POPC membrane samples used for <sup>2</sup>H NMR typically contained 22–25 mg of rhodopsin. The <sup>2</sup>H NMR spectra were acquired using a Bruker AMX 500 spectrometer with a narrow bore magnet (11.7 T). A custom-built high-power <sup>2</sup>H NMR probe was utilized, which was optimized for the rhodopsin-containing samples. A composite-pulse quadrupolar-echo sequence (135°<sub>x</sub>-90°<sub>x</sub>-45°<sub>-x</sub>- $\tau$ -135°<sub>y</sub>-90°<sub>-y</sub>-45°<sub>y</sub>- $\tau$ -acquisition) was employed and was phase-cycled to acquire the <sup>2</sup>H NMR signals. The delay  $\tau$  varied from 40 to 70  $\mu$ s and the recycle delay for the pulse sequence was typically 0.1–1.5 s. The membrane tilt angle was adjusted manually and was measured with a protractor.

Research was supported by U. S. National Institutes of Health grants GM 36564 (to K.N.) and EY 12049 (to M. F. B.). We thank Constantin Job, Avigdor Leftin, and Neil Jacobsen for assistance with the NMR experiments and helpful discussions. K.T. is grateful to the JSPS for the award of a Postdoctoral Fellowship for Research Abroad. G. F. J. S. received a predoctoral fellowship award from the BIO5 Institute of the University of Arizona. M. F. B. thanks the JSPS for the award of a Research Fellowship at the Institute for Protein Research.

## Appendix

**Modeling Retinal Conformation Bound to Receptor.** The possible orientations and structures of retinal based on NMR spectroscopy and linear dichroism data were obtained as follows. As a specific example we consider the metarhodopsin I state with an all-*trans* polyene chain. To calculate the orientation of retinal in the binding pocket of rhodopsin, we introduce the angle of the C9 methyl group to the bilayer normal as obtained by <sup>2</sup>H NMR. In addition we include the orientation of the main transition dipole moment obtained from linear dichroism studies of rhodopsin in either the dark state<sup>51</sup> or the meta I state.<sup>52</sup> These two axes define the orientation of the central B plane of the retinylidene moiety within the rhodopsin binding pocket. The orientations of the A and C planes are defined by the C5 and C13 methyl axes, respec-

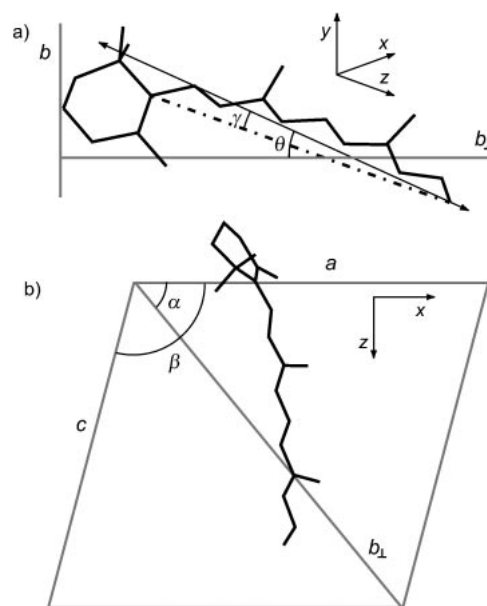


Fig. 5. Projection of the retinal molecule onto (a) the crystallographic (10 $\bar{1}$ ) plane and (b) the (010) plane. The retinal long axis is indicated by the broken line and the transition dipole moment by the solid line with double arrows (see text).

tively (cf. Fig. 4 of text). In both states, the transition dipole moment makes an angle of 16° to the membrane surface. However, we also need to know the orientation of the main transition dipole moment with respect to the retinal molecular axis. In the dark state this angle is found to be 16°, where the molecular axis for 11-*cis* retinal is chosen as the line connecting carbons C6 and C12.<sup>40</sup>

Now for the meta I state, referring to Fig. 5 the transition dipole moment orientation of *trans* retinal with respect to the molecular axis is determined by the angle  $\gamma$ , which is calculated from linear dichroism data<sup>53</sup> in combination with the corresponding X-ray crystal structure.<sup>54</sup> Figure 5a shows the projection of the retinal molecule within the crystal unit cell onto the (10 $\bar{1}$ ) plane, where the long axis of the retinal molecule is defined as a line connecting the C6 and O atoms. The double-headed arrow represents the main transition dipole moment ( $m$ ). The polyene chain plane is chosen as passing through the molecular axis and minimizes the distances of odd-numbered carbons including the C9 and C13 methyl groups from the plane. The transition dipole moment was assumed to lie in this plane and to form an angle  $\gamma$  with the long axis of the molecule.

Referring now to Fig. 5a, for a unit vector  $\mathbf{d}$  collinear with the transition moment we have:

$$\mathbf{d} = \mathbf{k} \cos \gamma + \mathbf{i} \sin \gamma. \quad (1)$$

Here,  $\mathbf{i}$  and  $\mathbf{k}$  are orthogonal unit vectors spanning the plane of the polyene chain, and the vector  $\mathbf{k}$  is collinear with the long molecular axis. Moreover, an axis  $\mathbf{b}_\perp$  is defined that is perpendicular to the monoclinic  $b$ -axis and placed in the (10 $\bar{1}$ ) plane. Next, in accord with Fig. 5b we can write:

$$\mathbf{b}_\perp = \mathbf{x} \cos \alpha + \mathbf{z} \sin \alpha, \quad (2)$$

where  $\mathbf{b}_\perp$  is a unit vector. Here  $\alpha$  is the angle the  $\mathbf{b}_\perp$ -axis makes with the  $x$ -axis of the Cartesian system, and  $(\mathbf{x}, \mathbf{y}, \mathbf{z})$  in are unit vectors referred to the orthogonal crystallographic axes ( $a, b, c^*$ ). The angle  $\alpha$  can be calculated from the parameters of

the unit cell ( $a = 15.270$ ,  $b = 8.264$ ,  $c = 14.942$  Å,  $\beta = 104.73^\circ$ ), giving:

$$\alpha = \tan^{-1} \left( \frac{c \sin \beta}{a - c \cos \beta} \right). \quad (3)$$

The acute angle  $\theta$  is between the projection of the transition moment  $m$  of the retinal molecule onto the  $(10\bar{1})$  plane, i.e. the plane of measurement, and the  $b_\perp$  axis, cf. Fig. 4a. It is determined from linear dichroism as:

$$\theta = \tan^{-1}(m_b/m_{b_\perp}) = \tan^{-1} \sqrt{P}, \quad (4)$$

where  $P \equiv m_b^2/m_{b_\perp}^2$  is the polarization ratio for the two directions  $b$  and  $b_\perp$ . Combining Eqs. 1, 2, and 4 and using  $m_b = m\mathbf{d} \cdot \mathbf{y}$  and  $m_{b_\perp} = m\mathbf{d} \cdot \mathbf{b}_\perp$  leads to:

$$\tan \theta = \frac{(\mathbf{k} \cos \gamma + \mathbf{i} \sin \gamma) \cdot \mathbf{y}}{(\mathbf{k} \cos \gamma + \mathbf{i} \sin \gamma) \cdot (\mathbf{x} \cos \alpha + \mathbf{z} \sin \alpha)}. \quad (5)$$

Hence, we arrive at the following result:

$$\gamma = \tan^{-1} \left( \frac{k_y - k_x \tan \theta \cos \alpha - k_z \tan \theta \sin \alpha}{i_x \tan \theta \cos \alpha + i_z \tan \theta \sin \alpha - i_y} \right). \quad (6)$$

The angle  $\theta$  has been reported<sup>53</sup> as  $24.1^\circ$ , from which one can derive that  $\gamma = 4.4^\circ$ . Knowing the orientation of the main transition dipole moment with respect to (i) the retinal long axis (angle  $\gamma$ ) and (ii) the membrane normal, together with (iii) the orientation of the C9 methyl group, one can determine the inclination of the retinal long axis to the membrane normal. In this way, for the dark and meta I states we obtain values of  $62$  and  $71^\circ$ , respectively.

The possible solutions (cf. Fig. 4 of text) for the *trans* polyene chain of retinal in meta I can then be calculated based on angular restraints obtained from  $^2\text{H}$ NMR for the C5 and C13 methyl groups<sup>37</sup> and distance constraints from  $^{13}\text{C}$  rotational resonance NMR.<sup>39,41</sup> In Fig. 4, structures (c) through (h) are excluded on account of the different position of the  $\beta$ -ionone ring with respect to retinal in the dark state.<sup>34</sup> These structures as well as structure (b) do not fit into the rhodopsin binding pocket in the dark state and have numerous steric clashes, leaving structure (a) as the physical solution.

## References

- # Dedicated to Professor Hideo Akutsu on the occasion of his retirement from the Directorship of the Institute for Protein Chemistry at Osaka University.
- 1 L.-Y. Lian, D. A. Middleton, *Prog. Nucl. Magn. Reson. Spectrosc.* **2001**, 39, 171.
- 2 H. Yagi, T. Tsujimoto, T. Yamazaki, M. Yoshida, H. Akutsu, *J. Am. Chem. Soc.* **2004**, 126, 16632.
- 3 O. C. Andronesi, S. Becker, K. Seidel, H. Heise, H. S. Young, M. Baldus, *J. Am. Chem. Soc.* **2005**, 127, 12965.
- 4 Y. Todokoro, I. Yumen, K. Fukushima, S.-W. Kang, J.-S. Park, T. Kohno, K. Wakamatsu, H. Akutsu, T. Fujiwara, *Biophys. J.* **2006**, 91, 1368.
- 5 A. P. Tulloch, *Prog. Lipid Res.* **1983**, 22, 235.
- 6 J. Lugtenburg, *Pure Appl. Chem.* **1985**, 57, 753.
- 7 S. Moltke, A. A. Nevzorov, N. Sakai, I. Wallat, C. Job, K. Nakanishi, M. P. Heyn, M. F. Brown, *Biochemistry* **1998**, 37, 11821.
- 8 G. Gröbner, I. J. Burnett, C. Glaubitz, G. Choi, A. J. Mason, A. Watts, *Nature (London)* **2000**, 405, 810.
- 9 E. Crocker, M. Eilers, S. Ahuja, V. Hornak, A. Hirshfeld, M. Sheves, S. O. Smith, *J. Mol. Biol.* **2006**, 357, 163.
- 10 M. F. Brown, in *Biological Membranes. A Molecular Perspective from Computation and Experiment*, ed. by K. Merz, Jr., B. Roux, Birkhäuser, Basel, **1996**, p. 175.
- 11 M. F. Brown, S. Lope-Piedrafita, G. V. Martinez, H. I. Petrache, *Modern Magnetic Resonance*, ed. by G. A. Webb, Springer, Heidelberg, **2006**, p. 245.
- 12 A. Watts, *Nat. Rev. Drug Discovery* **2005**, 4, 555.
- 13 M. E. Hatcher, D. L. Mattiello, G. A. Meints, J. Orban, G. P. Drobny, *J. Am. Chem. Soc.* **1998**, 120, 9850.
- 14 A. A. Nevzorov, S. Moltke, M. F. Brown, *J. Am. Chem. Soc.* **1998**, 120, 4798.
- 15 E. Endress, H. Heller, H. Casalta, M. F. Brown, T. Bayerl, *Biochemistry* **2002**, 41, 13078.
- 16 F. Seiff, J. Westerhausen, I. Wallat, M. P. Heyn, *Proc. Natl. Acad. Sci. U.S.A.* **1986**, 83, 7746.
- 17 M. P. Heyn, J. Westerhausen, I. Wallat, F. Seiff, *Proc. Natl. Acad. Sci. U.S.A.* **1988**, 85, 2146.
- 18 K. Nakanishi, R. Crouch, *Isr. J. Chem.* **1995**, 35, 253.
- 19 A. Wada, N. Fujioka, Y. Tanaka, M. Ito, *J. Org. Chem.* **2000**, 65, 2438.
- 20 A. F. L. Creemers, J. Lugtenburg, *J. Am. Chem. Soc.* **2002**, 124, 6324.
- 21 G. S. Harbison, S. O. Smith, J. A. Pardo, J. M. L. Courtin, J. Lugtenburg, J. Herzfeld, R. A. Mathies, R. G. Griffin, *Biochemistry* **1985**, 24, 6955.
- 22 V. Copié, A. E. McDermott, K. Beshah, J. C. Williams, M. Spyker-Assink, R. T. Gebhard, J. Lugtenburg, J. Herzfeld, R. G. Griffin, *Biochemistry* **1994**, 33, 3280.
- 23 A. S. Ulrich, I. Wallat, M. P. Heyn, A. Watts, *Nat. Struct. Biol.* **1995**, 2, 190.
- 24 S. O. Smith, I. Palings, M. E. Miley, J. Courtin, H. de Groot, J. Lugtenburg, R. A. Mathies, R. G. Griffin, *Biochemistry* **1990**, 29, 8158.
- 25 G. F. J. Salgado, A. V. Struts, K. Tanaka, N. Fujioka, K. Nakanishi, M. F. Brown, *Biochemistry* **2004**, 43, 12819.
- 26 M. R. Fransen, I. Palings, J. Lugtenburg, P. A. A. Jansen, G. W. T. Groenendijk, *Recl. Trav. Chim. Pays-Bas* **1980**, 99, 384.
- 27 G. Eyring, B. Curry, R. Mathies, R. Fransen, I. Palings, J. Lugtenburg, *Biochemistry* **1980**, 19, 2410.
- 28 M. F. Brown, *Curr. Top. Membr.* **1997**, 44, 285.
- 29 N. Fishkin, N. Berova, K. Nakanishi, *Chem. Rec.* **2004**, 4, 120.
- 30 A. V. Botelho, N. J. Gibson, Y. Wang, R. L. Thurmond, M. F. Brown, *Biochemistry* **2002**, 41, 6354.
- 31 A. A. Nevzorov, S. Moltke, M. P. Heyn, M. F. Brown, *J. Am. Chem. Soc.* **1999**, 121, 7636.
- 32 T. Okada, M. Sugihara, A.-N. Bondar, M. Elstner, P. Entel, V. Buss, *J. Mol. Biol.* **2004**, 342, 571.
- 33 H. Nakamichi, T. Okada, *Proc. Natl. Acad. Sci. U.S.A.* **2006**, 103, 12729.
- 34 A. V. Struts, G. F. J. Salgado, K. Tanaka, S. Krane, K. Nakanishi, M. F. Brown, *J. Mol. Biol.* **2007**, 372, 50.
- 35 Y. Fujimoto, N. Fishkin, G. Pescitelli, J. Decatur, N. Berova, K. Nakanishi, *J. Am. Chem. Soc.* **2002**, 124, 7294.
- 36 Y. Fujimoto, J. Ishihara, S. Maki, N. Fujioka, T. Wang, T. Furuta, N. Fishkin, B. Borhan, N. Berova, K. Nakanishi, *Chem. Eur. J.* **2001**, 7, 4198.
- 37 G. F. J. Salgado, A. V. Struts, K. Tanaka, S. Krane, K. Nakanishi, M. F. Brown, *J. Am. Chem. Soc.* **2006**, 128, 11067.
- 38 J. J. Ruprecht, T. Mielke, R. Vogel, C. Villa, G. F. X. Schertler, *EMBO J.* **2004**, 23, 3609.
- 39 P. J. R. Spooner, J. M. Sharples, S. C. Goodall, H. Sedorf,

- M. A. Verhoeven, J. Lugtenburg, P. H. M. Bovee-Geurts, W. J. deGrip, A. Watts, *Biochemistry* **2003**, *42*, 13371.
- 40 S. Jäger, J. W. Lewis, T. A. Zvyaga, I. Szundi, T. P. Sakmar, D. S. Kliger, *Proc. Natl. Acad. Sci. U.S.A.* **1997**, *94*, 8557.
- 41 P. J. E. Verdegem, P. H. M. Bovee-Geurts, W. J. de Grip, J. Lugtenburg, H. J. M. de Groot, *Biochemistry* **1999**, *38*, 11316.
- 42 P. J. R. Spooner, J. M. Sharples, M. A. Verhoeven, J. Lugtenberg, C. Glaubitz, A. Watts, *Biochemistry* **2002**, *41*, 7549.
- 43 K. Martínez-Mayorga, M. C. Pitman, A. Grossfield, S. E. Feller, M. F. Brown, *J. Am. Chem. Soc.* **2006**, *128*, 16502.
- 44 B. Borhan, M. L. Souto, H. Imai, Y. Shichida, K. Nakanishi, *Science* **2000**, *288*, 2209.
- 45 K. Palczewski, T. Kumasaka, T. Hori, C. A. Behnke, H. Motoshima, B. A. Fox, I. Le Trong, D. C. Teller, T. Okada, R. E. Stenkamp, M. Yamamoto, M. Miyano, *Science* **2000**, *289*, 739.
- 46 D. C. Teller, T. Okada, C. A. Behnke, K. Palczewski, R. E. Stenkamp, *Biochemistry* **2001**, *40*, 7761.
- 47 J. Li, P. C. Edwards, M. Burghammer, C. Villa, G. F. X. Schertler, *J. Mol. Biol.* **2004**, *343*, 1409.
- 48 J. W. Shriver, G. D. Mateescu, E. W. Abrahamson, *Biochemistry* **1979**, *18*, 4785.
- 49 A. Wada, M. Sakai, Y. Imamoto, Y. Shichida, M. Yamauchi, M. Ito, *J. Chem. Soc., Perkin Trans. 1* **1997**, 1773.
- 50 G. Gröbner, G. Choi, I. J. Burnett, C. Glaubitz, P. J. E. Verdegem, J. Lugtenberg, A. Watts, *FEBS Lett.* **1998**, *422*, 201.
- 51 P. A. Liebman, *Biophys. J.* **1962**, *2*, 161.
- 52 M. Chabre, J. Breton, *Vision Res.* **1979**, *19*, 1005.
- 53 G. Drikos, H. Rüppel, *Photochem. Photobiol.* **1984**, *40*, 93.
- 54 T. Hamanaka, T. Mitsui, T. Ashida, M. Kakudo, *Acta Crystallogr., Sect. B* **1972**, *28*, 214.